Near-infrared-activated gold nanoshells for thermal ablation of macrophages in vitro

Amani R. Makkouk[a], Henry Hirschberg[b], H. Michael Gach[c], and Steen J. Madsen[*a]

[a]Dept. of Health Physics, University of Nevada, Las Vegas, 4505 Maryland Pkwy., Box 453037, Las Vegas, NV 89154
[b]Beckman Laser Institute, University of California, Irvine, 1002 Health Sciences Rd. E, Irvine, CA 92612
[c]Nevada Cancer Institute, One Breakthrough Way, Las Vegas, NV 89135

ABSTRACT

In vitro studies were initiated to determine the suitability of murine and rat macrophages as delivery vehicles for gold nanoshells in the treatment of gliomas. Visualization of macrophage accumulation in and around gliomas may be accomplished using magnetic resonance imaging (MRI) and superparamagnetic iron oxide nanoparticles (SPIO). The optimal loading of both murine and rat macrophages with SPIO was determined using inductively coupled plasma atomic emission spectroscopy (ICP-AES). Higher concentrations of SPIO were observed in rat macrophages and the optimal concentration in these cell lines was around 300 μg/ml. Higher concentrations resulted in significant cell toxicity. SPIO were visualized in fixed rat brains subjected to high field MRI using T_2*-weighted gradient echo pulse sequences. Macrophages were found to be very sensitive to near infra-red (NIR) laser irradiation.

Keywords: Gold nanoshells, photothermal ablation, glioma, macrophages, superparamagnetic iron oxide nanoparticles

*steen.madsen@unlv.edu; phone: 702.895.1805; Fax: 702.895.4819

1. INTRODUCTION

Glioblastoma multiforme (GBM), classified by WHO as grade IV astrocytoma, is the most common type of glioma (50.7%) and the most malignant form of astrocytoma[1-4]. Its clinical history is usually less than three months in more than 50% of cases[5]. Despite the fact that the past 30 years have witnessed tremendous advances in diagnostics and multimodal treatments (surgery, radiotherapy and chemotherapy), the current median survival of GBM patients after first-line therapy is only 14.6 months [6-9].

Nanopartices are structures less than 500 nm in size which have sparked interest with their novel properties (optical, magnetic and thermal)[10-12]. Gold nanoshells represent one class of photo-absorbing nanoparticles[13, 14]. They consist of a spherical dielectric silica core (50-500 nm) surrounded by a thin (5–20 nm) gold layer[13, 15], and have a tunable optical absorption within the visible and infrared regions[13, 14]. They are being used for photothermal ablation of tumors[16, 17] using lasers with wavelengths at ~ 800 nm as the light source[15, 18, 19]. Following their intravenous injection, nanoshells can passively accumulate in the tumor through its leaky vasculature via a process known as enhanced permeability and retention (EPR)[13, 20].

Another class of nanoparticles which provide attractive magnetic resonance imaging (MRI) contrast agents is superparamagnetic iron oxide nanoparticles (SPIO), which consist of an iron oxide core encased in a hydrophilic dextran coating[10, 21, 22]. Clinically, SPIO are mainly used for with T2- and T2*-weighted sequences for tumor diagnosis[21, 23].

Macrophages are a class of phagocytic white blood cells[24, 25] that can be recruited by tumors (specifically hypoxic areas) via a chemoattractive gradient [26-28]. Macrophages infiltrating tumors are called tumor associated macrophages (TAMs)[27]. In GBM, regions of hypoxia are common, and TAMs can constitute up to a third of the tumor mass[29, 30]. Thus, they

Photonic Therapeutics and Diagnostics VI, edited by N. Kollias, B. Choi, H. Zeng, R. S. Malek, B. J.-F. Wong, J. F. R. Ilgner, K. W. Gregory, G. J. Tearney, L. Marcu, H. Hirschberg, S. J. Madsen, A. Mandelis, A. Mahadevan-Jansen, E. D. Jansen, Proc. of SPIE Vol. 7548, 754840 · © 2010 SPIE · CCC code: 1605-7422/10/$18 · doi: 10.1117/12.845553

represent attractive vehicles for the delivery of diagnostic or therapeutic agents such as nanoparticles[24, 26, 27, 31] because the EPR effect is insufficient when the goal is to accumulate nanoparticles within the central hypoxic region of the tumor (where resistant cells reside)[32].

The use of macrophages loaded with gold nanoshells for thermal ablation of GBM tumors is an attractive, relatively safe treatment modality that has not yet been explored. Another challenge lies in the addition of SPIO to the gold nanoshell-loaded macrophages for the purpose of MRI tracking of the macrophages following their systemic *in vivo* injection.

The feasibility of this approach is being studied in an *in vitro* model of glioma spheroids with the use of continuous wave (CW) laser light for ablation. In the present work, the optimal loading of macrophages with SPIO was determined, and the viability of unloaded macrophages exposed to NIR laser irradiation was studied.

2. MATERIALS AND METHODS

2.1 Cell lines and Nanoparticles

Two macrophage cell lines were used: the murine macrophage-like cell line P388D1 (ATCC# CCL-46) and rat alveolar macrophages NR8383 (ATCC# CRL-2192). For cancer cells, the rat glioma cell line C-6 (ATCC# CCL-107) was used. All cell lines were maintained in Dulbecco Modified Eagle Medium (DMEM) with high glucose (Invitrogen Corp., Carlsbad, CA, USA) supplemented with 10% fetal bovine serum (FBS), 25 mM HEPES buffer (pH 7.4), penicillin (100 U ml^{-1}) and streptomycin (100 µg ml^{-1}) at 37°C and 5% CO_2. C-6 cells were grown as monolayers, and a confluency of 70% was used in all experiments.

Feridex I.V® (Advanced Magnetics, Inc., Cambridge, MA, USA) was used for SPIO. It is a suspension of Ferumoxides (mean particle size of 58.5 nm) that delivers 11.2 mg Fe per ml. AuroShell™ particles (Nanospectra Biosciences Inc., Houston, TX, USA) were used for gold nanoshells. They are supplied as a suspension of bare gold nanoshells in deionized water at a concentration of 3.205 x 10^9 particles per ml.

2.2 MR imaging of Ferumoxides

Experiments were performed in a 7 T horizontal small bore scanner (Bruker, Billerica, MA, USA). Images were acquired *ex vivo* on a paraformaldehyde-fixed Fischer rat brain. Prior to imaging, 0.2 ml of Feridex® was injected directly into the excised brain. T_2*-weighted gradient echo MR pulse sequences (TR/TE = 1600/10 ms; flip angle = 30°, FOV = 35 mm; slice thickness = 1.0 mm) were used to detect the iron oxide particles.

2.3 Loading macrophages with Ferumoxides

Macrophages (2.5 x 10^6 cells for P388D1 and 1 x 10^6 cells for NR8383) were incubated with variable concentrations of Feumoxide for 24 hrs at 37°C in 5% CO_2. Cells incubated without Ferumoxides represented the blank. The amount of iron uptaken by the cells was quantified using inductively coupled plasma atomic emission spectrometry (ICP-AES). Briefly, cells were washed two times with phosphate-buffered saline (PBS) so as to remove all particles not endocytosed. Following centrifugation and counting, the cell number was adjusted to be the same in the blank and the samples, and the final cell pellet was transferred to an epitube and mineralized with 70% HNO_3 at 80°C for 1.5 hrs. 20 µl of 30% H_2O_2 were added, and then mineralization was presumed for another 3.5 hrs. Samples were then diluted with DI water to obtain a HNO_3 concentration of 5% in a 10 ml final volume, then filtered using a 0.45 µm membrane and stored at +4°C until ICP-AES analysis.

Samples were measured using an iCAP 6500 series (Thermo Scientific, Inc., Cambridge, UK) ICP-AES at λ = 238.2 nm. Calibration was performed with five standards prepared from SPEX CertiPrep Iron Standard (CAT# CLFE 2-2 Y) at concentrations of 0, 1, 2.5, 5, 15 and 25 ppm Fe in 5% HNO_3.

2.4 NIR laser irradiation of macrophages

Five thousand P388D1 macrophages in a total volume of 50 µl were transferred per well of a 384-well plate. 4 wells were used per group. Laser ablation was accomplished using a diode laser (Intense, North Brunswick, NJ, USA) at λ = 805.5 nm. The laser output power was calibrated with a Lasermate/D external power meter (Coherent, Santa Clara, CA, USA).Wells were irradiated with various power densities ranging from 1 to 10 W/cm^2, after which 50 µl of fresh media was added, and the cells were transferred to wells of a 96-well plate for colorimetric assay.

Following incubation for 24 hr, viability was assessed using the colorimetric MTS assay (Promega, USA). Briefly, each well was incubated with 20 µL of MTS/PMZ for 4 hr in a shaker at 37 °C and 50 rpm. Absorbance was then read at 490 nm with an Infinite M1000 plate reader (Tecan Systems Inc., San Jose, CA, USA). The percent viability of the cells was expressed as the ratio of absorbance of irradiated cells relative to that of non-irradiated cells (after subtracting the absorbance of the blank "medium" from each) multiplied by 100. A calibration curve was established using P388D1 cell densities of 0, 1250, 2500, 5000, 10000 and 25000 cells incubated with MTS/PMZ under similar conditions.

3. RESULTS

3.1 Ferumoxides can be clearly visualized *ex vivo* using MRI

The signal drop along the Ferumoxide injection tract is clearly visualized on the T_2*-weighted MR images, as depicted in Fig. 1 (arrow). The hypointense area could be detected for at least 30 minutes post-injection.

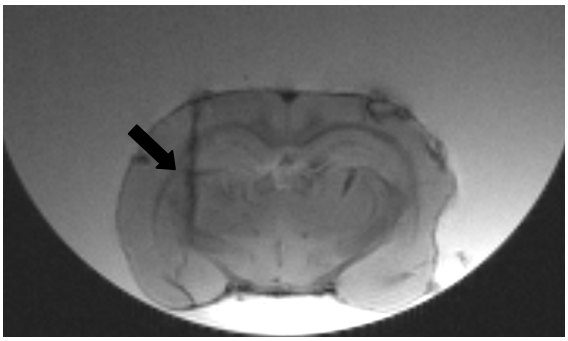

Figure 1. Visualization of the Ferumoxide injection tract (arrow). T_2*-weighted gradient echo MR image taken on a paraformaldehyde-fixed excised rat brain following the injection of 0.2 ml of Feridex®.

3.2 Uptake of Ferumoxides in macrophages is dose-dependent

Figure 2 shows a dose-dependent response of murine and rat macrophages respectively to increasing concentrations of Ferumoxides. It is also noticed that the amount of Ferumoxide uptaken in rat macrophages is much higher than that in murine macrophages, as is denoted by the much higher intracellular iron measured (over 50 fold at 400 µg/ml). One explanation for this observation is that rat macrophages generally have a higher endocytotic capacity. Higher Ferumoxide concentrations were not attempted due to cell toxicity already observed at 400 µg/ml. An optimal concentration of 300 µg/ml was chosen.

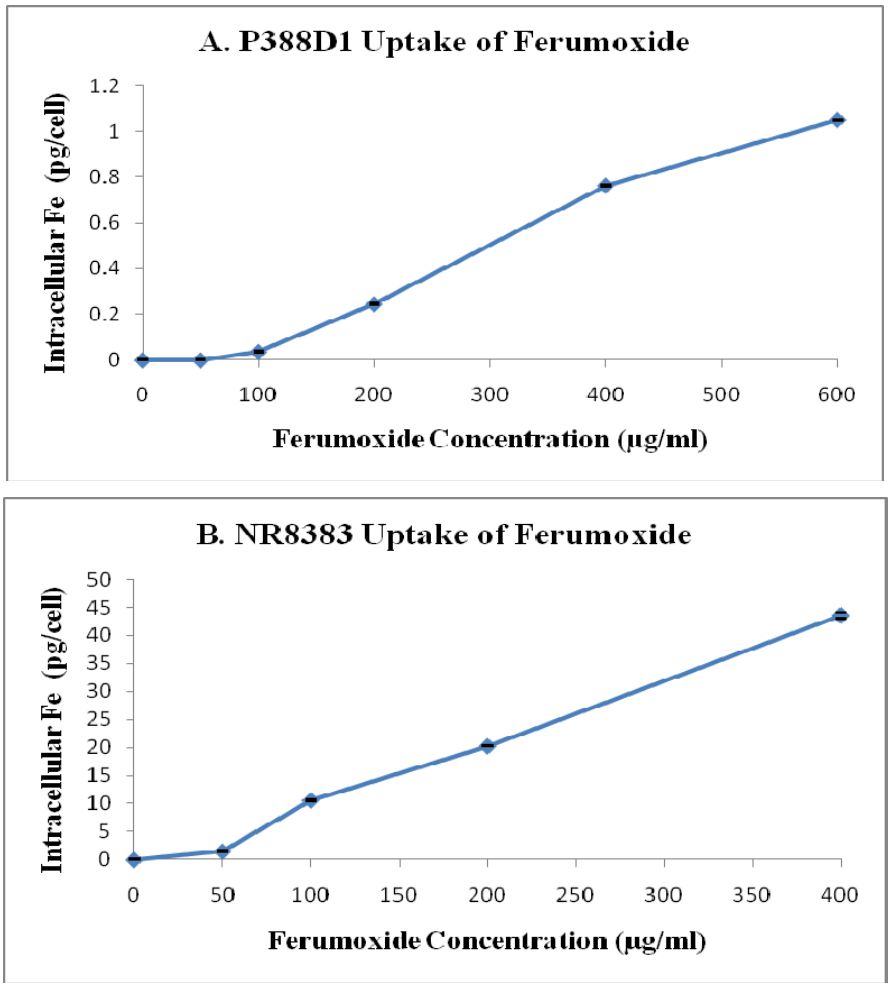

Figure 2. Dose-dependent internalization of Ferumoxide in murine (**A**) and rat (**B**) macrophages. Macrophages were incubated with Ferumoxide for 24 hr, and iron uptake was assessed by ICP-AES. Each point represents the mean of 4 experiments. Error bars (within points) denote standard deviations.

3.3 Macrophages are highly sensitive to NIR laser irradiation

NIR irradiation of murine macrophages resulted in a significant decrease in survival in a dose-dependent manner, as shown in Fig. 3.

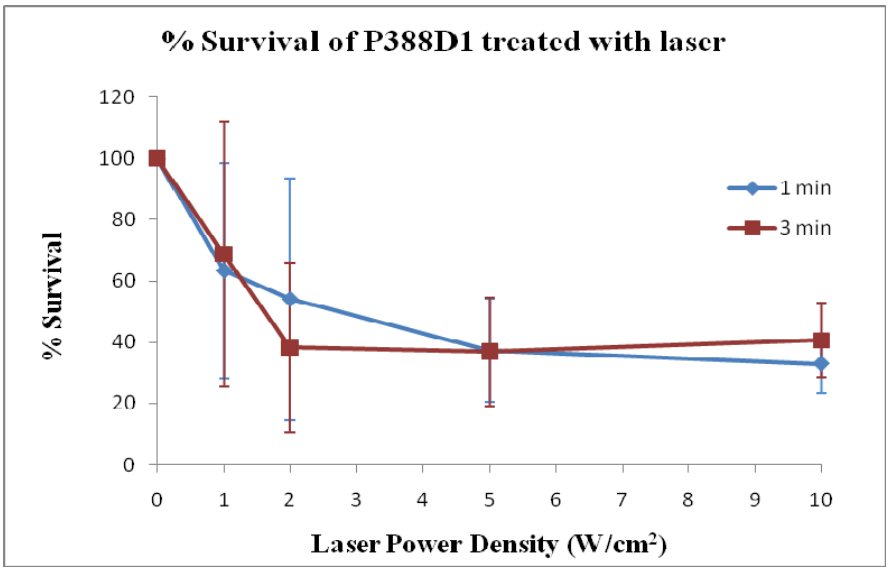

Figure 3. Response of murine macrophages to NIR laser irradiation. Each point represents the mean of 4 wells. Five thousand macrophages per well were irradiated at λ = 805.5 nm for 1 or 3 min. Percent survival was assessed 24 hr post-irradiation using the MTS assay. Error bars denote standard error.

4. DISCUSSION

The clinical use of Ferumoxides for the acquisition of T2*-weighted sequences is well documented[21]. Rather than observing agar suspensions of the Ferumoxides with MRI, we sought to visualize the particles in an *ex vivo* setting that can be better employed for future *in vivo* rat experiments. As expected, deposited Ferumoxides lowered the measured spin-spin relaxation time (T2*), producing negative enhancement along the injection tract.

ICP-AES quantitative analysis showed that Ferumoxide is incorporated by both murine and rat macrophages in a dose-dependent manner, in agreement with other published results involving SPIO and animal/human macrophages[25]. Several researchers have studied macrophage labeling with SPIO, and have so far shown that uptake is dependent on the cell and nanoparticle involved, in addition to experimental conditions such as SPIO concentration and incubation duration[33]. Variation in the intracellular iron content is thus expected, and our results show that high intracellular iron content was achieved for rat NR8383 macrophages at 100 µg/ml (43.56 pg/cell) versus only 0.76 pg/cell for murine P388D1 macrophages.

Siglienti et al. were able to obtain 4.33 pg Fe/cell following the incubation of rat peritoneal macrophages with 2 µM (112 µg Fe/ml) ferucarbotran (carboxydextran-coated SPIO) for 2 hr[34]. Even though ferucarbotran has, in principle, a higher cellular uptake due to its ionic surface coating[25], our results were much higher, possibly because of the longer incubation time (24 hr vs. 2 hr). On the other hand, Valable et al. were able to obtain 2.8 pg/cell following the incubation of murine P388D1macrophages with 62.8 µg Fe/ml MPIO (micrometer-sized particles of iron-oxide) for 18 hr[35]. Earlier reports have shown that larger-sized iron oxide particles are more efficiently phagocytosed[25], which explains why Valable et al. obtained a higher intracellular iron content for their 0.9-µm particles compared to our 58.5-nm Ferumoxides[36].

The irradiation of murine macrophages to increasing laser power densities resulted in a dose-dependent decrease in survival, as assessed by the colorimetric MTS/PMZ technique. It can thus be concluded that macrophages, as vehicles carrying the nanoparticles, can be thermally ablated very easily at relatively low laser densities and even in the absence of laser-activated nanoshells.

Bernardi et al. have shown that glioma cells require much higher laser power densities for photoablation with nanoparticles[37]. They used an output of 80 W/cm^2 for 2 min from an 800-nm NIR laser. Consequently, it is expected that

using such a high laser output for nanoshell activation will result in immediate ablation of the nanoshell-loaded macrophages and the release of their cargo of laser-activated nanoshells onto glioma cells. In other words, the use of macrophages as vehicles is not expected to hinder the function of loaded nanoshells as tumor-ablating tools.

5. CONCLUSIONS

The results of the present study show that the uptake of ferumoxides is dose-dependent in both murine and rat macrophages, and that Ferumoxides can be visualized *ex vivo* in rat brains via the acquisition of T_2*-weighted MR images. The high sensitivity of macrophages to NIR laser irradiation suggests that their use as vehicles for carrying the nanoshells to the tumor is not going to hinder the tumor-ablative function of the nanoshells.The aim of ongoing work is to evaluate the use of doubly-loaded macrophages thermal ablation of *in vitro* glioma spheroids.

ACKNOWLEDGMENTS

The authors are grateful for the support of the Nevada System of Higher Education Health Sciences System which sponsored this research through the Inter-institutional Biomedical Research Fund (NSHE #09-x32).

REFERENCES

[1] Gomez GG, Kruse CA. Mechanisms of malignant glioma immune resistance and sources of immunosuppression. Gene Ther.Mol.Biol. 2006;10(A):133-146.

[2] Maru SV, Holloway KA, Flynn G, Lancashire CL, Loughlin AJ, Male DK, et al. Chemokine production and chemokine receptor expression by human glioma cells: role of CXCL10 in tumour cell proliferation. J.Neuroimmunol. 2008 Aug 13;199(1-2):35-45.

[3] Chandana SR, Movva S, Arora M, Singh T. Primary brain tumors in adults. Am.Fam.Physician 2008 May 15;77(10):1423-1430.

[4] La Rocca RV, Mehdorn HM. Localized BCNU chemotherapy and the multimodal management of malignant glioma. Curr.Med.Res.Opin. 2009 Jan;25(1):149-160.

[5] Yamanaka R. Cell- and peptide-based immunotherapeutic approaches for glioma. Trends Mol.Med. 2008 May;14(5):228-235.

[6] Selznick LA, Shamji MF, Fecci P, Gromeier M, Friedman AH, Sampson J. Molecular strategies for the treatment of malignant glioma--genes, viruses, and vaccines. Neurosurg.Rev. 2008 Apr;31(2):141-55; discussion 155.

[7] Maier-Hauff K, Rothe R, Scholz R, Gneveckow U, Wust P, Thiesen B, et al. Intracranial thermotherapy using magnetic nanoparticles combined with external beam radiotherapy: results of a feasibility study on patients with glioblastoma multiforme. J.Neurooncol. 2007 Jan;81(1):53-60.

[8] Sathornsumetee S, Rich JN. Designer therapies for glioblastoma multiforme. Ann.N.Y.Acad.Sci. 2008 Oct;1142:108-132.

[9] Martin V, Liu D, Gomez-Manzano C. Encountering and advancing through antiangiogenesis therapy for gliomas. Curr.Pharm.Des. 2009;15(4):353-364.

[10] Cuenca AG, Jiang H, Hochwald SN, Delano M, Cance WG, Grobmyer SR. Emerging implications of nanotechnology on cancer diagnostics and therapeutics. Cancer 2006 Aug 1;107(3):459-466.

[11] Roco MCE-. Nanoparticles and Nanotechnology Research. Journal of Nanoparticle Research 1999 03/01/;1(1):1-6.

[12] Euliss LE, DuPont JA, Gratton S, DeSimone J. Imparting size, shape, and composition control of materials for nanomedicine. Chem.Soc.Rev. 2006 Nov;35(11):1095-1104.

[13] Hirsch LR, Gobin AM, Lowery AR, Tam F, Drezek RA, Halas NJ, et al. Metal nanoshells. Ann.Biomed.Eng. 2006 Jan;34(1):15-22.

[14] Huang X, Qian W, El-Sayed IH, El-Sayed MA. The potential use of the enhanced nonlinear properties of gold nanospheres in photothermal cancer therapy. Lasers Surg.Med. 2007 Oct;39(9):747-753.

[15] Zharov VP, Kim JW, Curiel DT, Everts M. Self-assembling nanoclusters in living systems: application for integrated photothermal nanodiagnostics and nanotherapy. Nanomedicine 2005 Dec;1(4):326-345.

[16] Huang Y, Sefah K, Bamrungsap S, Chang H, Tan W. Selective Photothermal Therapy for Mixed Cancer Cells Using Aptamer-Conjugated Nanorods. Langmuir 2008 10/21;24(20):11860-11865.

[17] Huang X, Jain PK, El-Sayed IH, El-Sayed MA. Determination of the minimum temperature required for selective photothermal destruction of cancer cells with the use of immunotargeted gold nanoparticles. Photochem.Photobiol. 2006 Mar-Apr;82(2):412-417.

[18] Terentyuk GS, Maslyakova GN, Suleymanova LV, Khlebtsov NG, Khlebtsov BN, Akchurin GG, et al. Laser-induced tissue hyperthermia mediated by gold nanoparticles: toward cancer phototherapy. J.Biomed.Opt. 2009 Mar-Apr;14(2):021016.

[19] Liu C, Mi CC, Li BQ. Energy absorption of gold nanoshells in hyperthermia therapy. IEEE Trans.Nanobioscience 2008 Sep;7(3):206-214.

[20] Zaman RT, Diagaradjane P, Wang JC, Schwartz J, Rajaram N, Gill-Sharp KL, et al. In Vivo Detection of Gold Nanoshells in Tumors Using Diffuse Optical Spectroscopy. Selected Topics in Quantum Electronics, IEEE Journal of 2007;13(6):1715-1720.

[21] Neumaier CE, Baio G, Ferrini S, Corte G, Daga A. MR and iron magnetic nanoparticles. Imaging opportunities in preclinical and translational research. Tumori 2008 Mar-Apr;94(2):226-233.

[22] Thorek DL, Chen AK, Czupryna J, Tsourkas A. Superparamagnetic iron oxide nanoparticle probes for molecular imaging. Ann.Biomed.Eng. 2006 Jan;34(1):23-38.

[23] Park K, Liang G, Ji X, Luo Z, Li C, Croft MC, et al. Structural and Magnetic Properties of Gold and Silica Doubly Coated γ-Fe2O3 Nanoparticles. The Journal of Physical Chemistry C 2007 12/01;111(50):18512-18519.

[24] Owen MR, Byrne HM, Lewis CE. Mathematical modelling of the use of macrophages as vehicles for drug delivery to hypoxic tumour sites. J.Theor.Biol. 2004 Feb 21;226(4):377-391.

[25] Metz S, Bonaterra G, Rudelius M, Settles M, Rummeny EJ, Daldrup-Link HE. Capacity of human monocytes to phagocytose approved iron oxide MR contrast agents in vitro. Eur.Radiol. 2004 Oct;14(10):1851-1858.

[26] Murdoch C, Lewis CE. Macrophage migration and gene expression in response to tumor hypoxia. Int.J.Cancer 2005 Dec 10;117(5):701-708.

[27] Knowles HJ, Harris AL. Macrophages and the hypoxic tumour microenvironment. Front.Biosci. 2007 May 1;12:4298-4314.

[28] Choi MR, Stanton-Maxey KJ, Stanley JK, Levin CS, Bardhan R, Akin D, et al. A cellular Trojan Horse for delivery of therapeutic nanoparticles into tumors. Nano Lett. 2007 Dec;7(12):3759-3765.

[29] Flynn JR, Wang L, Gillespie DL, Stoddard GJ, Reid JK, Owens J, et al. Hypoxia-regulated protein expression, patient characteristics, and preoperative imaging as predictors of survival in adults with glioblastoma multiforme. Cancer 2008 Sep 1;113(5):1032-1042.

[30] Kennedy BC, Maier LM, D'Amico R, Mandigo CE, Fontana EJ, Waziri A, et al. Dynamics of central and peripheral immunomodulation in a murine glioma model. BMC Immunol. 2009 Feb 18;10:11.

[31] Beduneau A, Ma Z, Grotepas CB, Kabanov A, Rabinow BE, Gong N, et al. Facilitated monocyte-macrophage uptake and tissue distribution of superparmagnetic iron-oxide nanoparticles. PLoS ONE 2009;4(2):e4343.

[32] Lal S, Clare SE, Halas NJ. Nanoshell-enabled photothermal cancer therapy: impending clinical impact. Acc.Chem.Res. 2008 Dec;41(12):1842-1851.

[33] Hsiao JK, Chu HH, Wang YH, Lai CW, Chou PT, Hsieh ST, et al. Macrophage physiological function after superparamagnetic iron oxide labeling. NMR Biomed. 2008 Oct;21(8):820-829.

[34] Siglienti I, Bendszus M, Kleinschnitz C, Stoll G. Cytokine profile of iron-laden macrophages: implications for cellular magnetic resonance imaging. J.Neuroimmunol. 2006 Apr;173(1-2):166-173.

[35] Valable S, Barbier EL, Bernaudin M, Roussel S, Segebarth C, Petit E, et al. In vivo MRI tracking of exogenous monocytes/macrophages targeting brain tumors in a rat model of glioma. Neuroimage 2008 Apr 1;40(2):973-983.

[36] Varallyay P, Nesbit G, Muldoon LL, Nixon RR, Delashaw J, Cohen JI, et al. Comparison of two superparamagnetic viral-sized iron oxide particles ferumoxides and ferumoxtran-10 with a gadolinium chelate in imaging intracranial tumors. AJNR Am.J.Neuroradiol. 2002 Apr;23(4):510-519.

[37] Bernardi RJ, Lowery AR, Thompson PA, Blaney SM, West JL. Immunonanoshells for targeted photothermal ablation in medulloblastoma and glioma: an in vitro evaluation using human cell lines. J.Neurooncol. 2008 Jan;86(2):165-172.